Here $aB/2\pi$ is the amplitude of the interrow periodic potential, G is the mean force due to adjacent layers [0 and 3 in Fig. 2(d)] and f_i are fluctuating forces. Requiring $\langle\dot{\phi}\rangle_t \equiv 0$ leads at low temperature to $G = \{[v^2 + (B\mu)^2]^{1/2} - v\}/\mu$ and $\langle\sigma^2\rangle_t = 4\mu G v$, where $\langle\sigma^2\rangle_t$ is a measure of the roughness of the sliding of the rows relative to each other. The transition region corresponds to $v = B\mu$ or a characteristic shear rate $S_c = B\mu/a$, at which G begins to drop and $\langle\sigma^2\rangle_t$ is near maximum. For $B \sim Ea^2 \sim 10^{-8}$ dyn, $\mu = (6\pi\eta r)^{-1} \sim 10^5$ dyn cm/sec, and $a \sim 10^{-4}$ cm, we find $S_c \sim 10$ Hz, in good qualitative agreement with our observations.

A mechanism for transition I is suggested by the structuring of the $k_v > 0$ lines into spots. The spots become more diffuse, especially in the $\hat{k}_e$ direction with increasing $\hat{k}_v$, indicating a broadening arising from transverse lattice vibrations with displacement $\vec{\alpha}$ along $\hat{k}_v$ and wave vector $\vec{q}$ along $\hat{k}_e$ in the 2D hcp sheets as shown in Fig. 2(a). This broadening and hence the 2D lattice vibration amplitude increases with increasing shear rate. As a model for intraplane transverse phonon generation, we considered a layer to be an isotropic elastic membrane subjected to a random thermal force and a drag force due to the local fluid velocity. A displacement in the $\hat{\nabla}$ direction couples to a motion in $\hat{v}$ direction and leads to a larger rms absolute displacement of a point or relative displacement of two points as the shear is increased. The allowed wavelengths in this calculation must be bounded from below by a limit on the number of possible states and from above as well, giving a "size" to the plates within a layer. To satisfy a Lindemann criterion the plates shrink as the shear increases, in agreement with observation. Details of these arguments will be published elsewhere.

One of us (B. J. A.) acknowledges support from the Research Corporation.

[1]R. Williams and R. S. Crandall, Phys. Lett. 48A, 225 (1974).
[2]N. A. Clark, A. J. Hurd, and B. J. Ackerson, Nature 281, 57 (1979).
[3]R. Williams, R. S. Crandall, and P. J. Wojtowicz, Phys. Rev. Lett. 37, 348 (1976).
[4]N. A. Clark and B. J. Ackerson, Phys. Rev. Lett. 44, 1005 (1980).
[5]J. M. Ziman, *Principles of the Theory of Solids*, (Cambridge Univ. Press, Cambridge, 1964), p. 63.
[6]T. Schneider, E. P. Stoll, and R. Morf, Phys. Rev. B 18, 1417 (1978).
[7]S. E. Trullinger, M. D. Miller, R. A. Guyer, A. R. Bishop, F. Palmer, and J. A. Krumhansl, Phys. Rev. Lett. 40, 206, 1603(E) (1978).

Soliton Propagation in ^{3}He-*A*

T. J. Bartolac, C. M. Gould, and H. M. Bozler
Department of Physics, University of Southern California, Los Angeles, California 90007
(Received 12 September 1980)

A propagating magnetic texture has been observed in superfluid ^{3}He-*A* confined to 17-μm slabs with use of pulsed NMR. The results support a model of an expanding lattice of solitons in the order parameter. The propagation velocity approaches the spin-wave velocity as $T \to T_c$, and goes to zero for $T < 0.86T_c$. Despite the narrow geometry, the solitons observed involve distortions of both the spin and orbital degrees of freedom.

PACS numbers: 67.50.Fi, 61.16.Hn, 75.30.Ds

We report the first measurements of a propagating spin-related mode in superfluid ^{3}He-*A*. This work was stimulated by the proposals of Maki and co-workers[1-3] that solitons can exist in the superfluid, and by the successful observation of these metastable textures by several groups.[4-7] Perhaps the most intriguing aspect of solitons is the prediction that they can propagate through the superfluid. We have observed this propagation and find that near T_c the velocity approaches the calculated spin-wave velocity,[8] but decreases at lower temperatures, going to zero for $T/T_c < 0.86$.

The metastable modes in ^{3}He-*A* have been found to be most reliably produced by pulsed transverse NMR, and most easily identified by a change in the NMR frequency. In ^{3}He-*A* this frequency obeys the relation[2,7]

$$\omega^2 = (\gamma H_0)^2 + (R_T \Omega_A)^2, \quad (1)$$

where γH_0 is the Larmor frequency, Ω_A is the longitudinal resonance frequency, and R_T^2 is a constant ($0 \leq R_T^2 \leq 1$) which depends upon the type of texture (soliton) present. We have taken a novel approach to observing the propagation of this

magnetic mode by observing the influence that the texture has on the transverse resonance frequency instead of directly measuring the amplitude of the magnetization of the fluid.

In order to enhance the possibility of observing soliton propagation, the superfluid was confined to the 17-μm spaces separating a stack of 51 sapphire sheets (each 19×0.05 mm^3). The purpose of the narrow spacing was to prevent motion by the gap anisotropy axis, $\hat{l}$, which obeys a rigorous boundary condition that it be normal to all solid walls. We expected that by holding $\hat{l}$ fixed, the dissipation which motion of $\hat{l}$ always produces[9] would be eliminated, thereby allowing solitons to propagate relatively freely. However, the evidence from our experiments indicates that, contrary to our expectations, major distortions of the $\hat{l}$ texture do occur, even in the 17-μm geometry.

Figure 1(a) shows a single slab of ^{3}He and the relative orientations of the static and rf magnetic fields. Surrounding the ^{3}He were two collinear coils, each controlled by a separate pulsed NMR system. The rf fields from the two coils overlap only weakly, as shown in Fig. 1(a), thus minimizing the mutual interaction of the coils. Furthermore, while one coil was pulsed, ringing in the other coil was prevented both by detuning it and by applying a small "bucking" pulse. The static magnetic field (168 G) was in the plane of the ^{3}He slabs, so that the initial "uniform" texture (when dipole and bending energies are simultaneously minimized) would have both $\hat{l}$ and $\hat{d}$ (the susceptibility anisotropy axis) normal to the planes.

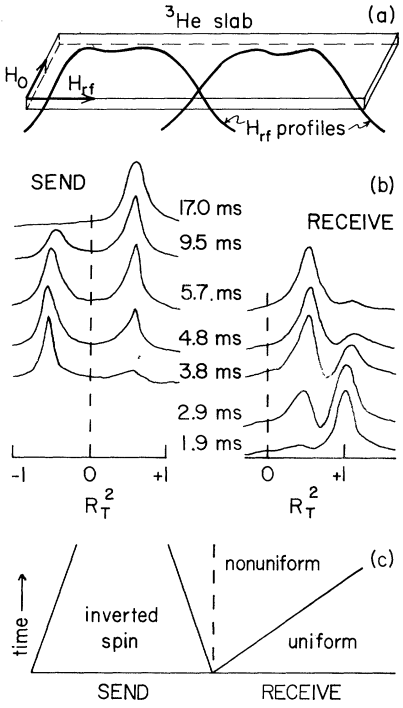

FIG. 1. (a) Geometry of the experiment showing the orientation of the static and rf magnetic fields relative to the ^{3}He sample, along with the rf-field profiles. The receive coil's half-power points are 1.00 ± 0.02 cm apart. (b) Experimentally observed NMR results and (c) the model used to interpret them. The curves in (b) are Fourier transforms of FID signals in both the send coil (on the left) and receive coil (on the right) at various times following the 180° pulse in the send coil.

Following the same method known to create textures in bulk fluid, we applied a 180° rf pulse to one coil (the "send" coil), inverting the spin inside that coil, followed after a chosen time delay by a small rf probe pulse (~18°) to the "receive" coil. The resulting free-induction-decay signal (FID) from the receive coil was captured with a transient recorder and stored in a computer.[7] We then restored the uniform texture in the fluid by thermally cycling the ^{3}He through the normal phase. At each temperature explored, the basic sequence (180° pulse–delay–18° pulse–thermal cycle) was repeated with delays of 1.92, 2.86, 3.81, 4.75, and 5.69 ms. The resulting FID's display the evolution of a propagating texture as if caused by a single spin inversion.

Typical results for this evolution are shown in Fig. 1(b). Here we plot the Fourier transform of the FID signals to demonstrate the qualitative behavior of the superfluid. However, because of the rapid time evolution of the textures, the actual analysis utilized the original FID signals. The curves on the left are from the send coil and show the decay of the negatively shifted signal associated with spin inversion as seen in previous experiments.[6,7] In this paper we consider the signals seen in the receive coil. The data presented here were taken at a pressure of 25.25 bars; however, additional data at 23.06 and 28.66 bars showed no significant pressure dependence.

Immediately after the 180° pulse the superfluid in the receive coil is unaffected. After a short delay, however, a portion of the "uniform" signal at $R_T^2=1$ is transformed to a lower frequency. Eventually the entire signal is converted to the lower frequency. A simple model which we have used to describe this process is shown in Fig. 1(c). We assume that following the 180° pulse in the send coil, a nonuniform texture with some $R_T^2<1$ emerges from that coil and moves into the receive coil at a constant velocity, destroying the

uniform fluid at $R_T^2 = 1$.

We determine the soliton velocity not by estimating the time when solitons first reach the receive coil, but rather by analyzing the entire transformation from uniform to nonuniform fluid in the receive coil. The several FID's, each with a duration of several milliseconds, provide in effect a continuous record of the instantaneous frequencies in the coil. We use numerical curve-fitting procedures to simultaneously fit each complete sequence of FID's with the model described above. The model requires that the phase of the spin precession is continuous at any point in the fluid as the soliton lattice moves down the coil. Despite its simplicity we find that the resulting computer fit agrees with the original set of FID's to within 3% at each point. The frequency resolution is better than 20 Hz. The errors in the velocity come primarily from the simplicity of the model. (For example, the solitons' velocity is probably changing as they pass through the receive coil.) By testing the sensitivity of the fit to the velocity, we estimate that this measurement is accurate to ~5%.

Figure 2(a) shows the temperature dependence of the observed propagation velocity, v, compared with the appropriate spin-wave velocity,[8] $c_{s\perp}$. We see that although v does not exhibit a strong temperature dependence, it does stay below $c_{s\perp}$ for all temperatures, and eventually decreases at lower temperatures. Since the spin-wave velocity is a characteristic velocity of the superfluid, it is perhaps more useful to plot the ratio $v/c_{s\perp}$ as a function of temperature as in Fig. 2(b). We obtain an excellent straight-line fit, $v/c_{s\perp} = 0.825 - 6.06(1 - T/T_c)$, suggesting that propagation should not occur when $1 - T/T_c > 0.136$. Indeed, observations made at $1 - T/T_c = 0.151$ demonstrated that a single spin inversion in the send coil was not sufficient to generate a nonuniform texture in the receive coil.

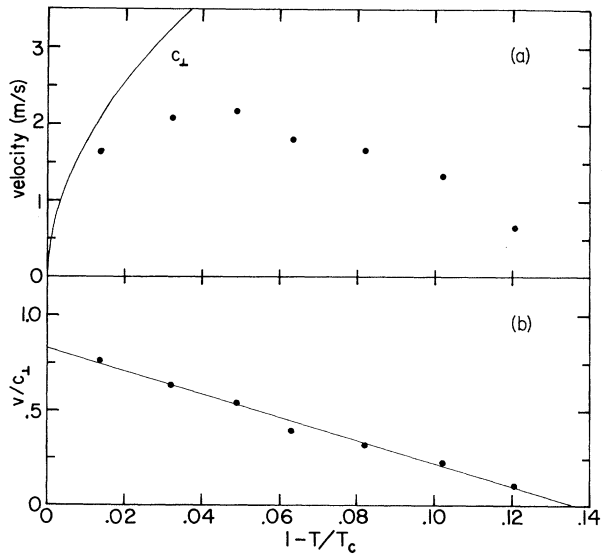

FIG. 2. (a) Temperature dependence of the propagation velocity at 25.25 bars, compared with the spin-wave velocity, $c_{s\perp}$. (b) Ratio of the propagation velocity to the spin-wave velocity as a function of temperature, with the best linear fit.

As the region with nonuniform texture moves into the receive coil, its NMR frequency increases with time as shown in Fig. 3(a). We note that during propagation, R_T^2 rapidly approaches ~0.55, relaxing faster at lower temperatures. The value of R_T^2 then adopts a much slower relaxation rate, generally reaching ~0.70 after ~10 s. Typical data over the longer time regime are shown in Fig. 3(b).

We interpret our results in terms of the soliton model of Maki and co-workers.[1-3] A soliton in superfluid ^{3}He-A is a texture of $\hat{l}$ and $\hat{d}$, with variation along only one dimension, which forms an interface (typically 10 μm thick) smoothly joining a region where $\hat{l} = +\hat{d}$ with a region where $\hat{l} = -\hat{d}$.

A "pure-$\hat{d}$" soliton results when $\hat{d}$ alone rotates 180° against a uniform $\hat{l}$ background, while a "composite" soliton results from $\hat{d}$ and $\hat{l}$ counter-rotating 180°. If many solitons are created, as is thought to occur in our experiments, they form

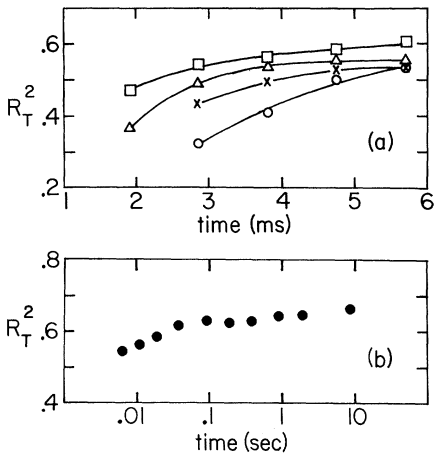

FIG. 3. (a) Short-term time dependence of R_T^2 in the propagating texture at 25.25 bars and $1 - T/T_c = 0.032$ (open circles), 0.049 (crosses), 0.063 (open triangles), and 0.102 (open squares). (b) Long-term time dependence of R_T^2 at 23.06 bars and $1 - T/T_c = 0.063$.

a one-dimensional soliton lattice, with the energy per soliton inversely proportional to the intersoliton spacing. Because of this mutual repulsion the solitons move apart. Moving solitons have a relativistic energy, $E(v) \simeq E_0[1-(v/c_{s\perp})^2]^{-1/2}$; thus the maximum possible soliton velocity is the spin-wave velocity. Finally, solitons are identified by their NMR frequency, given by Eq. (1). For example,[3] a composite soliton lattice has R_T^2 ranging between 0.55 (compressed limit) and 0.70 (dilute limit). In contrast, all pure-$\hat{d}$ solitons (whether isolated or in a lattice) show $R_T^2 = 0$.

In our experiments a large number of solitons are created by inverting the magnetization in the send coil with a 180° pulse. When the magnetization is inverted the spin equations of motion show that $\hat{d}$ rotates in the plane perpendicular to $\vec{H}_0$ at twice the Larmor frequency. This rotation occurs only in the send coil; the magnetization in the receive coil is intially unaffected. Thus a relative winding of $\hat{d}$ between the two coils is generated in the form of a dense pure-$\hat{d}$ soliton lattice. In all previous experiments on bulk ^{3}He-A this lattice was seen both to expand and (through some presently unknown mechanism) to acquire a certain amount of winding in $\hat{l}$, forming a composite soliton lattice.[6,7] The present experiment directly measures this expansion. Confining liquid to 17-μm slabs was an attempt to stabilize $\hat{d}$ solitons against decay into composite solitons.

Our first experimental conclusion is that since $R_T^2 \neq 0$, we do not have a pure-$\hat{d}$ soliton lattice. The soliton must involve $\hat{l}$ in spite of the large $\hat{l}$ bending energies between thin slabs, and in spite of the expectation that $\hat{d}$ motion during propagation would be too fast for the viscous $\hat{l}$ response. One would expect the propagation velocity and R_T^2 relaxation to be influenced by $\hat{l}$ motion. Because $\hat{l}$ damping increases with decreasing temperature,[9,10] the propagation velocity as measured in the receive coil should similarly decrease. In fact, for temperatures below $1 - T/T_c \sim 0.07$, we do find such a decrease, as shown in Fig. 2(a). Moreover, the ratio $v/c_{s\perp}$ in Fig. 2(b) shows a montonic decrease at all temperatures.

However, if the above ideas on $\hat{l}$ motion are correct, then we should also expect the transformation of pure-$\hat{d}$ solitons into composite solitons to occur at a slower rate at lower temperatures. This transformation is monitored by R_T^2 because, generally speaking, the more that $\hat{l}$ rotates through the soliton, the larger R_T^2 will be. Therefore, the rate at which R_T^2 increases directly measures the rate at which $\hat{d}$ solitons deform into composite solitons. Figure 3(a), however, shows R_T^2 increasing faster at lower temperatures, contrary to our expectations. We have not resolved this discrepancy.

Finally, we point out a long-standing problem in understanding solitons in ^{3}He-A, about which this experiment provides more information. Previous experiments[6,7] in bulk ^{3}He-A have seen the expansion of soliton lattices with R_T^2 increasing from 0.55 to 0.7. These frequencies agree with calculations done for the mainly $\hat{l}$ composite soliton lattice in which most of the relative winding is done by $\hat{l}$. However, since $\hat{d}$ is the vector being driven by the inverted magnetization, we would expect most of the winding to be done by $\hat{d}$, forming a mainly $\hat{d}$ soliton lattice. These two types of lattices are topologically distinct. Thus, although the mainly $\hat{l}$ texture has less energy than the mainly $\hat{d}$, it seems unlikely that one could decay into the other. Because the present experiment also sees R_T^2 evolve from 0.55 to 0.7, we conclude that whatever mechanism is responsible for transferring net winding out of $\hat{d}$ into $\hat{l}$ in bulk fluid must also be operable even when ^{3}He-A is confined between 17-μm-spaced walls.

We acknowledge useful discussions with K. Maki, R. Bruinsma, and Y. R. Lin-Liu. This work was supported by the National Science Foundation through Grant No. DMR-79-00830.

[1]K. Maki and P. Kumar, Phys. Rev. B 14, 118 (1976).

[2]K. Maki and P. Kumar, Phys. Rev. Lett. 38, 557 (1977), and Phys. Rev. B 16, 182 (1977).

[3]R. Bruinsma and K. Maki, Phys. Rev. B 20, 984 (1979).

[4]R. W. Giannetta, E. N. Smith, and D. M. Lee, Phys. Lett. 62A, 335 (1977).

[5]J. Kokko, M. A. Paalanen, R. C. Richardson, and Y. Takano, J. Phys. C 11, L125 (1978).

[6]H. M. Bozler and T. Bartolac, in *Physics of Ultra-low Temperatures*, edited by T. Sugawara *et al.* (Physical Society of Japan, Tokyo, 1978), p. 136; H. M. Bozler and T. J. Bartolac, Phys. Lett. 71A, 75 (1979).

[7]C. M. Gould, T. J. Bartolac, and H. M. Bozler, J. Low Temp. Phys. 39, 291 (1980).

[8]The spin-wave velocity is anisotropic. The maximum velocity, $c_{s\perp}$, measured when $\hat{l}$ is perpendicular to the propagation, is related to the fourth-sound velocity by $c_{s\perp}^2/c_4^2 = (1+F_0^a)/(1+F_0)$ [A. J. Leggett, Rev. Mod. Phys. 47, 331 (1975)]. Values for c_4 are obtained from H. Kojima, D. N. Paulson, and J. C. Wheatly, J. Low Temp. Phys. 21, 283 (1975).

[9]M. C. Cross and P. W. Anderson, in *Low Temperature Physics, LT-14*, edited by M. Krusius and M. Vuorio (American Elsevier, New York, 1975), Vol. I, p. 29.
[10]D. N. Paulson, M. Krusius, and J. C. Wheatley, Phys. Rev. Lett. 36, 1322 (1976).

Inelastic Light Scattering in a Onefold-Coordinated Amorphous Semiconductor

B. V. Shanabrook and J. S. Lannin
Department of Physics, The Pennsylvania State University, University Park, Pennsylvania 16802

and

I. C. Hisatsune
Department of Chemistry, The Pennsylvania State University, University Park, Pennsylvania 16802
(Received 19 May 1980)

The first measurements on low-temperature–deposited thin-film a-I are reported. *In situ* Raman spectra indicate that a-I is a onefold-coordinated semiconductor in contrast to other amorphous solids studied to date. The spectra surprisingly differ from those of molecular systems, indicating appreciable intermolecular coupling. Considerable structural disorder is indicated by a fivefold increase in intramolecular bandwidth relative to c-I. Delocalized bonding rather than weak directional covalent interactions is suggested for intermolecular coupling in a-I.

PACS numbers: 63.50.+x, 61.40.Df, 78.30.Gt

Of central importance in the study of amorphous solids is the role of nearest-neighbor coordination. Studies of amorphous semiconductors have focused on systems of low coordination number, $n_1 = 2$, 3, or 4. We report here on the formation of an amorphous solid with *minimum* coordination, onefold-coordinated amorphous (a) iodine. The Raman scattering spectra presented here represent the first physical measurements on a onefold-coordinated amorphous solid. Such a system is of special character as it may allow a separation of short-range, first-neighbor effects from second- and higher-neighbor interactions. This may be seen in an amorphous solid, since first-neighbor bond-length fluctuations are quite small and do not contribute appreciably to structural disorder. Thus the absence of bond-angle fluctuations, $\Delta\theta$, for $n_1 = 1$ implies that the origin of disorder is beyond the first coordination sphere. This is shown schematically in Fig. 1, where the atom at the center of the first coordination sphere for $n_1 > 1$ experiences variations in local electronic potential as well as in noncentral forces that result from fluctuations in θ.

In the crystalline (c) state, iodine is of special interest as a layered material in which both molecular and semiconducting characters are present.[1-4] The molecular character is exhibited by a narrow high-frequency band of intramolecular stretching modes and low-frequency lattice modes,[1] while the intermolecular separation of less than twice the van der Waals radius and nuclear quadrapole resonance indicate significant intermolecular coupling.[4] In c-I it has often been suggested that the intermolecular coupling between I_2 molecules has a directional character and involves local p-orbital interactions.[4,5] It might thus be expected that a-I would be more molecular in character as structural disorder should modify orbital orientational relationships. The Raman and depolarization spectra presented below do not indicate this expected behavior. This result is attributed to the combined role of appreciable disorder and nondirectional, delocalized bonding.[6] The results indicate that such bonding is a preferable description of the pre-

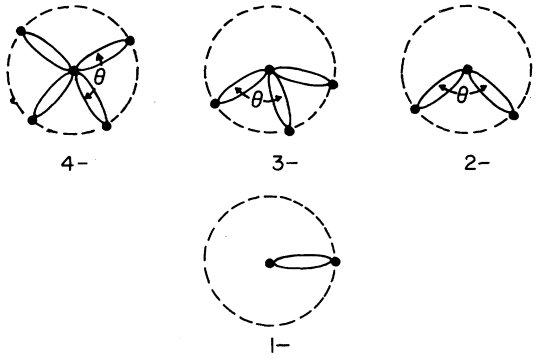

FIG. 1. Schematic of the nearest-neighbor bonding in elemental amorphous semiconductors within the first coordination sphere.